Edge-enhanced imaging obtained with very broad energy band x-rays

A. Taibi,[1] P. Cardarelli,[1] G. Di Domenico,[1] M. Marziani,[1] M. Gambaccini,[1,a)] T. Hanashima,[2] and H. Yamada[3]
[1]*Department of Physics, University of Ferrara, INFN Section of Ferrara, via Saragat 1, 44100 Ferrara, Italy*
[2]*Photon Production Laboratory Ltd., 1-1-1 Nojihigashi, Kusatsu, Shiga 525-8577, Japan*
[3]*Synchrotron Light Life Science Center, Ritsumeikan University, 1-1-1 Nojihigashi, Kusatsu, Shiga 525-8577, Japan*

(Received 27 November 2009; accepted 16 March 2010; published online 6 April 2010)

We demonstrate both theoretically and experimentally that edge-enhancement effects are produced when objects, in contact with the x-ray detector, are imaged by using very broad x-ray spectra. Radiographs of thin Al objects have been obtained with a table-top synchrotron source which generates x-rays in the energy range from a few kilo-electron-volts up to 6 MeV. Edge-enhancement effects arise from the combination of x-ray absorption (kilo-electron-volt part of the spectrum) and secondary particle emission (mega-electron-volt part of the spectrum) within the sample. The exact contribution of absorption and emission profiles in the edge-enhanced images has been calculated via Monte Carlo simulation. © *2010 American Institute of Physics*. [doi:10.1063/1.3380641]

Recently, several small-scale synchrotron light sources have been proposed, whereby the most advanced system is the MIRRORCLE, marketed by the Photon Production Laboratory, Ltd. (Japan).[1] Within the seventh framework program of the European Commission, a three-year project called *Labsync* has been recently funded with the aim to design a multipurpose small facility around the MIRRORCLE source.[2] The medical physics group of Ferrara University is one of the seven partners of the *Labsync* consortium.

The MIRRORCLE-6X source consists of two compact rings of about 60 cm of diameter; a microtron-type injector and a storage ring. The injector accelerates electrons up to 6 MeV with a peak current of 100 mA. The second ring stores the electron beam accelerated by the microtron at constant energy, with a current up to 2 A. Depending on which target is employed, a different x-ray beam can be obtained. Hard x-rays, mostly bremsstrahlung from a few kilo-electron-volts up to the electron energy, have been generated with a thin foil or wire target (10 μm–1 mm).[3,4] Figure 1 shows the production of a divergent x-ray beam after the interaction of the electrons circulating in the storage ring with a wire target inserted in the electron path. The angular divergence of the photon beam is about $1/\gamma$ where γ is the Lorenz factor of the electron. For a 6 MeV electron $1/\gamma \approx 85$ mrad.

The transport of 6 MeV electrons in a thin molybdenum, rhodium, and tungsten wire was studied in detail by means of Monte Carlo simulations using MCNPX.[5] It was shown that the emitted x-ray beams can be much more intense than those generated by conventional x-ray tubes for radiography applications (see Fig. 2). An experimental study was also carried out at the Photon Production Laboratory in Japan to evaluate the potential of the MIRRORCLE system in the field of diagnostic radiology. We utilized target materials similar to those studied in the Monte Carlo simulation; Mo wire 125 μm thick, Rh wire 120 μm thick, and W wire 125 μm thick. X-ray images of test objects were obtained by making use of the RadEye2 digital x-ray detector (Radicon Imaging Corp., USA) which is based on a Gd_2O_2S scintillator (Kodak Min-R 2190) coupled to a complementary metal-oxide-semiconductor (CMOS) photodiode array. The coating density of the phosphor is 34 mg/cm^2 (see Ref. 6) while the depletion region of the diode is about 3–5 μm of thickness.[7] The RadEye2 module is also packaged with a 1-mm-thick graphite window and the nominal range for detecting x-rays is 10–50 kV. The digital detector was placed at a distance of 1480 mm from the x-ray source. At this distance the radiation field entirely covers the detector surface.

The x-ray imaging experiment revealed an interesting effect of edge enhancement. As an example, Fig. 3 shows the edge of a polymethyl methacrylate (PMMA) slab 10-mm-thick. The PMMA sample was imaged by using a Mo wire 125 μm thick as target material. The x-ray contrast of PMMA in air, calculated in regions far from the edge, is only 3.5% while the *edge* contrast is more than 20%.

Such result is in agreement with the findings of Yamada and co-workers.[8] They discovered for the first time this effect by imaging, with the same MIRRORCLE source, sample plates in contact with the x-ray detector. Here, we provide a full explanation of the phenomenon by studying the various interactions of photons and electrons with matter. The well-known EGSnrc code system for the Monte Carlo simulation of photon and electron transport was used to carry out the study.[9] More specifically, we simulated the passage of a

FIG. 1. (Color online) Simulation of x-ray production within the storage ring.

a)Electronic mail: gambaccini@fe.infn.it.

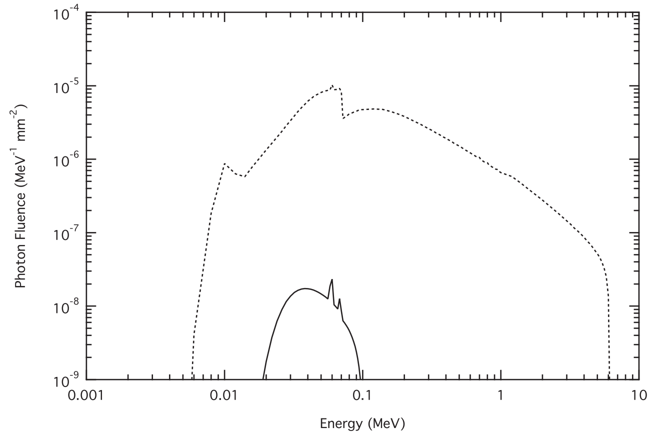

FIG. 2. Comparison of x-ray spectra emitted by a standard x-ray tube at 100 kV (continuous curve) and the MIRRORCLE-6X source (dotted curve). The fluence is given in units of photons per MeV per mm^2 per incident electron.

photon beam in a finite, right cylindrical geometry via the DOSRZnrc code. Since the code scores the energy deposited within user defined regions, we were able to calculate the charge collected in the digital detector so as to simulate the radiographic signal. The various layers used for modeling the interaction of the x-rays within the detector are shown in Fig. 4 (an air gap 3 mm thick was also included). The energy absorbed in the scintillator was converted into light and the charge generated in the diode by the number of emitted light photons was added to the charge produced by direct energy deposition within the Si layer. The image profile along the direction perpendicular to the disk edge was generated by using a fine sampling distance.

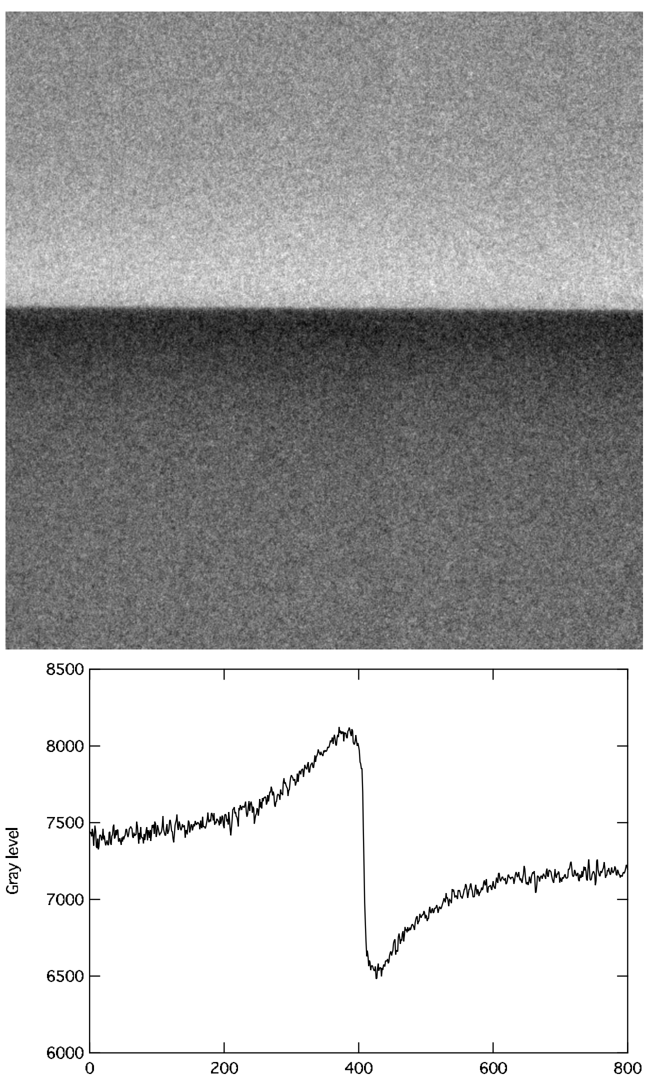

FIG. 3. (Top image) Radiograph of PMMA slab 10-mm-thick. The slab covers the bottom half of the x-ray detector. (Bottom image) The vertical profile shows the edge-enhancement effect.

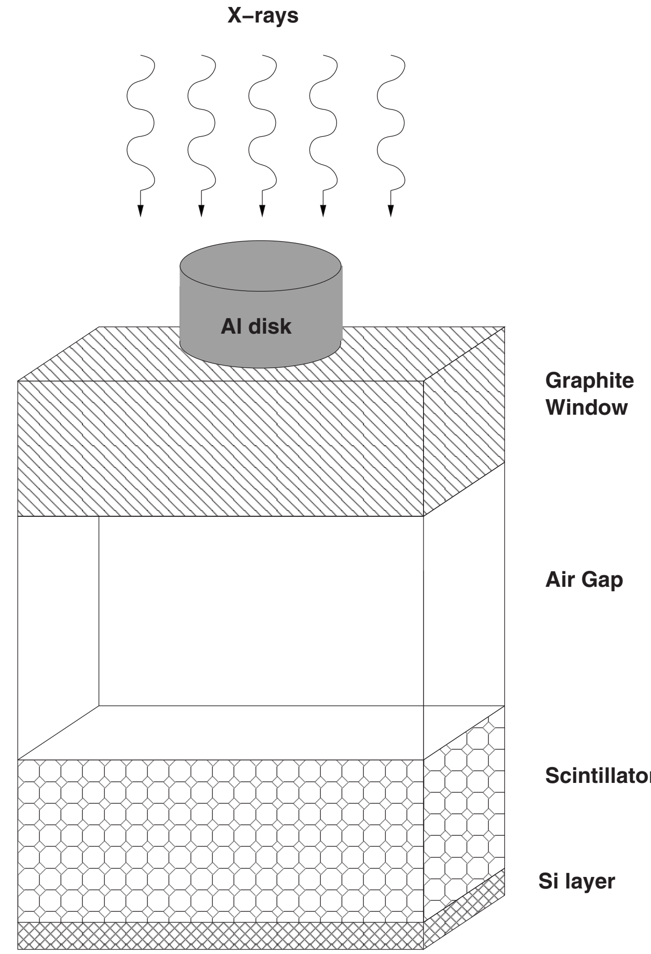

FIG. 4. Schematic of the x-ray interaction within the RadEye2 detector (not to scale).

Figure 5 shows the excellent agreement between a line profile taken from a radiograph of an Al detail 1 mm thick and the one obtained by means of the simulation. In this case a W wire 125 μm thick was used as target material.

Edge-enhancement effects arise from the combination of x-ray absorption and emission of electrons and photons within the sample. The relative contribution of primary and secondary radiation to image formation process has been quantified by splitting the input x-ray spectrum in three parts; 1–150 keV, 150 keV–1 MeV, and 1–6 MeV, respectively. Results of the simulation reveal that, in the case of an Al detail 1 mm thick, the edge-enhancement effect is due to the superposition of the 1–150 keV and 1–6 MeV profiles (see Fig. 6). Indeed, the low-energy spectrum provides the usual image contrast generated by the difference in x-ray attenuation between the object and the background. Due to the long source-to-detector distance, the x-ray penumbra is negligible so the profile changes abruptly at the edge of the Al disk. On the contrary, the image contrast provided by the high-energy

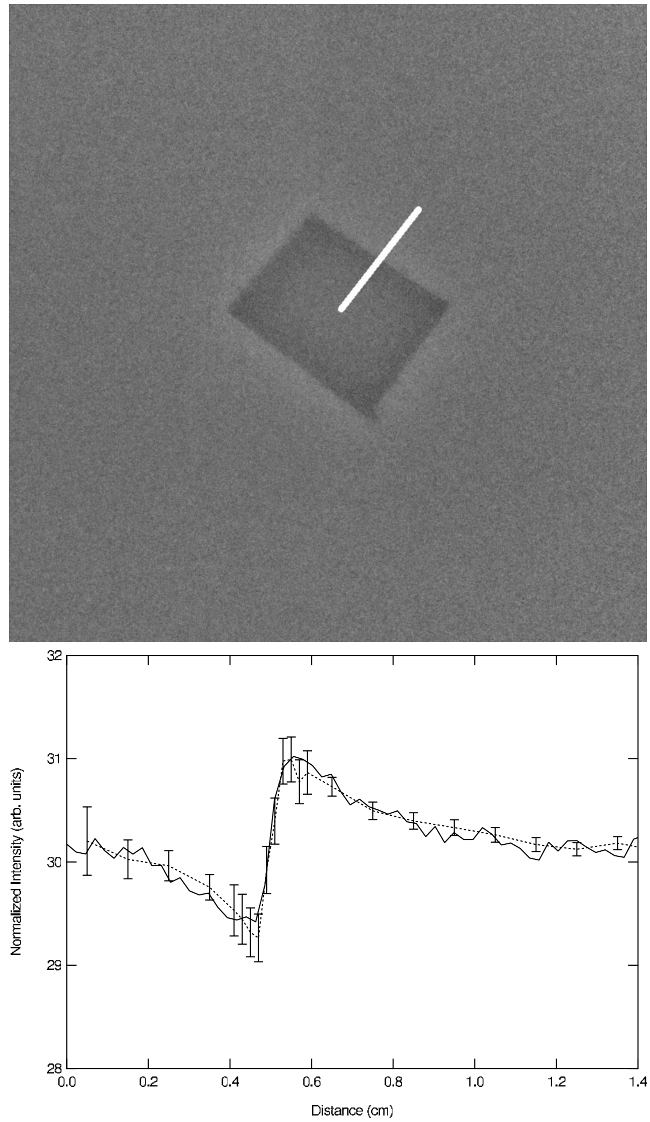

FIG. 5. Edge-enhancement effect: comparison between experimental and simulated data. The experimental data (continuous line) were taken from the radiograph of an Al detail (In the top image the white line represents the line profile used for the comparison). Data from the Monte Carlo simulation (dotted line) are reported with their statistical uncertainty.

spectrum is reversed because the x-ray detector is weakly sensitive to the primary radiation within this energy range and the signal is formed by secondary electrons and/or secondary photons of lower energy which are produced by the interaction of high-energy x-rays with the object. In this case, secondary particles scatter within the Al material and then penetrate the detector, thus spreading out the edge of the disk signal according to their range in matter. There is also a

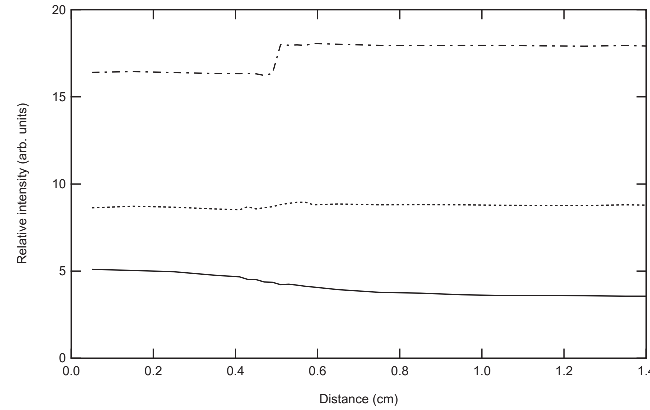

FIG. 6. Comparison of simulated line profiles obtained with three different x-ray spectra. 1–150 keV (dotted-dashed line), 150 keV–1 MeV (dotted line), and 1–6 MeV (continuous line).

broad energy range, from 150 keV to 1 MeV, in which the image contrast vanishes, i.e., the contribution of primary and secondary radiation is equally weighted.

We have shown that edge-enhancement effects which arise with objects in contact with the x-ray detector are due to the combination of x-ray absorption and secondary particle emission within the sample. Monte Carlo simulation not only provides full explanation of the phenomenon but also allows one to explore means for modulating it by changing both the relative contribution of the various parts of the very broad x-ray spectrum and the overall response of the imaging detector to radiation. Finally, depending on the x-ray imaging application with the MIRRORCLE source (radiological, nondestructive testing, etc.), an optimization of detector characteristics to either amplify or mitigate such effects is desirable.

The LABSYNC project (Laboratory compact light sources) has been funded by the European Commission under the Seventh Framework Programme (Grant No. 213126) "FP7-INFRASTRUCTURES."

[1] http://www.photon-production.co.jp/e/PPL-HomePage.html
[2] http://www.kuleuven.be/labsync/
[3] H. Yamada, T. Hirai, M. Morita, T. Hanashima, M. Sasaki, D. Hasegawa, T. Hayashi, T. Yamada, and H. Saisho, IPAP Conf. Ser. **7**, 130 (2006).
[4] H. Yamada, AIP Conf. Proc. **902**, 11 (2007).
[5] M. Marziani, A. Taibi, G. Di Domenico, and M. Gambaccini, Med. Phys. **36**, 4683 (2009).
[6] A. Taibi, in *Ionizing Radiation Detectors for Medical Imaging*, edited by A. Del Guerra (World Scientific, Singapore, 2004).
[7] T. Achterkirchen, Rad-icon Imaging Corp., personal communication (30 September 2009).
[8] T. Hirai, S. Maki, Y. Sonoda, H. Yamada, M. Sasaki, and D. Hasegawa, AIP Conf. Proc. **716**, 132 (2004).
[9] http://www.irs.inms.nrc.ca/inms/irs/EGSnrc/EGSnrc.html